The capabilities of the Theseus space mission for probing dark matter

Lindita Hamolli,[a,*] **Mimoza Hafizi,**[a] **Esmeralda Guliqani**[b] **and Marsida Laze**[c]

[a]*Department of Physics, University of Tirana,*
Boulevard "Zogu I", Tirana, Albania

[b]*Department of Mathematics and Physics, "Fan S. Noli" University of Korça,*
Street "Nënë Tereza", Ish-Divizioni, Korça, Albania

[c]*Department of Physics, "Aleksandër Xhuvani" University of Elbasan,*
Street "Ismail Zyma", Elbasan, Albania
E-mail: lindita.hamolli@fshn.edu.al, mimoz.hafizi@fshn.edu.al,
eguliqani@unkorce.edu.al, marsida.laze@uniel.edu.al

We explore the capability of IRT-Theseus to detect dark matter through strong lensing of quasars. Quasars, though compact, are very bright and distant objects with complex structures. Their lensing by foreground galaxies is significant in cosmology. By measuring the positions of the images, the time delay between them, and the magnification ratio, we can constrain the mass distribution of the lensing galaxy, refine cosmological parameters, and understand the physics of quasars. Using updated IRT-Theseus AB magnitude data and the Quasar Luminosity Function (QLF) from the Spitzer Space Telescope, we estimate that IRT will observe approximately $N \simeq 2.7 \times 10^5$ quasars with a redshift limit of $z = 4.5$. Additionally, we find that one in every 2500 quasars observed by IRT will be lensed. We also examine the microlensing effect in Broad Emission Lines (BELs). With a spectral resolution of (R=400) and photometric accuracy of 5%, we find that IRT-Theseus can detect microlensing in BELs, enhancing our understanding of quasar physics and the mass distribution of foreground galaxies.

COSMICWISPers2024,
3-6 September 2024,
Istinye University, Istanbul, Turkey.

*Speaker

1. Introduction

The nature of dark matter (DM) remains one of the most intriguing questions in cosmology and particle physics. Approximately 85% of the universe's matter is non-baryonic dark matter, inferred through gravitational effects. The existence of DM is supported by various observations, including the cosmic microwave background, galaxy rotation curves, galaxy cluster dynamics, and gravitational lensing (see [1] and references herein). Despite extensive observations, the physical nature of DM remains unsolved. Recent efforts have focused on both particle dark matter [2] and macroscopic dark matter, including localized point-like objects such as primordial black holes [3]. Analyses of microlensing events observed by OGLE over a 20-year period have constrained the fraction of primordial black holes in the Milky Way halo, suggesting they could constitute up to 10% of the total dark matter [4]. These objects are expected to alter the line profile at a rate consistent with microlensing in lensed quasars, which exhibit flux ratio anomalies. Beyond point-like macroscopic dark matter, theories suggest extended configurations, and gravitational lensing is a promising method to probe their substructures. WIMPs and axions, as candidates for Cold Dark Matter (CDM), are crucial for cosmic structure formation. Low-mass halos form first and merge over time to create larger structures like galaxies and clusters. Numerical simulations have detailed CDM halo properties. Recent research explains flux ratio anomalies in strongly lensed quasars using subhalo structures, showing that considering subhalos within the lensing galaxy and along the line of sight provides a better fit to observed data [5]. Consequently, lensed quasar events offer a promising opportunity to constrain various subhalo models, especially with upcoming surveys like the Large Synoptic Survey Telescope (LSST) and the Roman space telescope [6]. Section 2 discusses strong lensing and its role in DM detection. Section 3 examines the IRT Theseus's potential to detect lensed quasars. Section 4 summarizes our findings and conclusions.

2. Exploring dark matter through strong lensing

Gravitational lensing occurs when light rays from a distant source are bent by the gravitational potential of a foreground object, reaching the observer. This phenomenon offers a promising method to constrain dark matter within the Milky Way and on a larger cosmic scale. The study of dark matter in the Milky Way Halo involves microlensing observations toward the LMC, SMC, and M31. Investigations beyond our galaxy rely on strong lensing events. In strong lensing, due to the very large angular diameter distances between the observer and the lens (D_L), the observer and the source (D_S) and the lens and the source (D_{LS}), the mass of the lens is represented as a two-dimensional mass sheet lying perpendicular to the line of sight. The image positions ($\vec{\theta}$) are determined by the lens equation: $\vec{\beta} = \vec{\theta} - \vec{\alpha}(\vec{\theta})$, where $\vec{\beta}$ is the source position and $\vec{\alpha}(\vec{\theta})$ is the scaled deflection angle given by the gradient of the gravitational potential Ψ of the lens [7]. When $\vec{\beta} = 0$, the lens and the source are perfectly aligned, and the image is given by the Einstein ring radius θ_E, which is $\theta_E = \sqrt{\frac{4GM(\theta)}{c^2} \frac{D_{LS}}{D_S D_L}}$. Here, $M(\theta)$ is the total matter inside the Einstein radius. For a image at angular position θ, the magnifications determined by the inverse of the determinant of the Jacobian matrix: $\mu(\theta) = \left(\det \frac{\partial \vec{\beta}}{\partial \vec{\theta}} \right)^{-1} = \frac{1}{(1-\kappa)^2 - \gamma^2}$, where κ is the dimensionless surface density and γ corresponds to the shear. Both κ and γ determined by the second derivative of the lensing potential, depend on the mass model of the lens [7]. When a light ray from a distant source passes through the gravitational potential, Ψ of a massive object, it undergoes time dilation due to the Shapiro effect

[8]. Additionally, because the ray is bent, it requires more time to propagate compared to the direct path. The total time delay for a specific image cannot be measured due to the unknown position of the source. However, the relative time delay between two lensed images (1,2) can be calculated by: $\Delta t_{1,2} = \frac{1+z_L}{c} \frac{D_L D_S}{D_{LS}} \left[\frac{1}{2}(\vec{\theta}_1 - \vec{\beta})^2 - \frac{1}{2}(\vec{\theta}_2 - \vec{\beta})^2 - \Psi(\vec{\theta}_1) + \Psi(\vec{\theta}_2) \right]$. This depends on the distances, source position, image positions, and the strength of the gravitational potential. Consequently, all measurements—positions of images, their magnifications, and the time delays—rely on the mass distribution along the line of sight. In strong lensing, the source can be a quasar or a galaxy. Lensed quasars, due to their variability and brightness, provide high measurement accuracy and detailed information on dark matter distribution in the lensing galaxy. Although quasars are compact sources, they have a complex structure. At the center lies a supermassive black hole, which consumes a large amount of matter through an accretion disk. Farther away, there is the broad emission region (BER) and then the dusty torus [9]. Due to temperature variations, quasars emit radiation across the entire spectrum, from gamma rays to radio waves. Generally, the disk emits in optical and near-infrared (NIR), the broad emission region in infrared (IR), and the torus in mid-IR. In photometric and spectrometric observations of strongly lensed quasars, the microlensing effect is present. This effect is caused by objects within the lensing galaxy or along the line of sight, leading to additional magnification of the lensed images. Microlensing is particularly sensitive when the size of the source regions is comparable to or smaller than the Einstein radius in the source plane. More compact (and hotter) regions exhibit more distinguishable microlensing variability, resulting in chromatic behavior [9]. Generally, the accretion disk is microlensed by the stellar populations of the lensing galaxy. However, other regions, such as the broad emission region (BER) and the torus, can also be microlensed by subhalos. To distinguish the effects of subhalo structures in the lensing galaxy or along the line of sight, infrared (IR) and radio observations are preferred. This approach helps avoid the microlensing effect caused by the stellar population.

3. Lensed quasars with IRT-Theseus

To date, over 220 lensed quasars have been identified[1], but only a few provide sufficient measurements. We explore the use of IRT-Theseus to detect lensed quasars and the microlensing effect on them. THESEUS, (the Transient High Energy Survey and Early Universe Surveyor), is a multi-instrument mission to detect and characterize Gamma-Ray Bursts (GRBs) up to cosmological distances, and monitor the transient X-ray Universe. THESEUS payload will include three scientific instruments: Soft X-ray Imager (SXI, 0.3 - 5 keV), X-Gamma rays Imaging Spectrometer (XGIS, 2 keV – 10 MeV) and InfraRed Telescope (IRT). IRT is a 0.7 m class telescope with 15×15 arcmin FOV, with both imaging and spectroscopy capabilities in the $0.7 - 1.8$ μm band [10]. The IRT spectral resolution is R=400, and angular accuraly 1 arcsec. While primarily designed to study GRB afterglows detected by SXI or XGIS, IRT-THESEUS will also collect data on extragalactic sources like quasars. THESEUS will trigger observations with other facilities. To calculate the number of quasars expected to be observed by the IRT, we integrate the QLF (see [6] and refs herein) found by Lacy et al. [11] using the infrared band observations from the Spitzer Space Telescope imaging surveys. We provide updates compare to [12]: the AB magnitude in the H band has improved from 20.6 to 20.8, and the minimum luminosity is now given by $L_{min} = L_\odot 10^{\left(-18.444 - log \frac{23.04 \times 10^{-24}}{D_L^2} \right)}$,

---

[1]https://research.ast.cam.ac.uk/lensedquasars/

where D_L is the luminosity distance of the quasar. Since the IRT-THESEUS will cover 64% of the sky, we estimate that it will observe approximately $N \simeq 2.7 \times 10^5$ with a limit redshift of, $z = 4.5$. To determine the number of lensed quasars detected by IRT-Theseus, we use the same algorithm as in Hamolli et al, [6] with updated redshift distributions from the Milliquas catalog [13]. We generated a sample of 200,000 events using the redshift distributions of quasars and galaxies, along with galactic mass distribution and stellar velocity dispersion. Assuming the SIS model for galaxies, we calculate the probability of a quasar being lensed by one or more foreground galaxies. With IRT-Theseus's angular resolution of 1", we find that approximately one in every 2500 quasars observed by Roman is expected to be lensed. Our analysis also shows that about 90% of these configurations involve one foreground galaxy. Fig. 1: On the left, the redshift distributions of galaxies and quasars expected to be observed by IRT-Theseus are shown. The redshift range for galaxies is from 0 to 1.2, while for quasars, it spans from 0.8 to 4.5. On the right, the time delay distribution of strong lensing events is depicted, ranging from days to years, with the highest probability around several months. The bin width in the log scale is 0.1. Fian et al., [14] analyzed
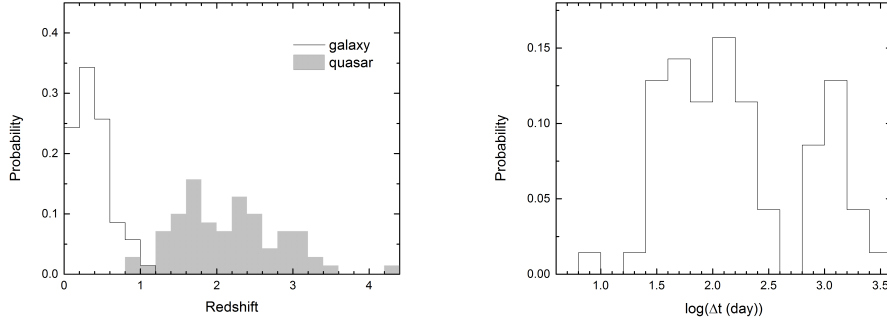

Figure 1: Left: Redshift distributions for galaxies (black line) and quasars (gray shadow). Right: Time delay distribution of strong lensing events.

27 lensed quasars and found that the microlensing variability of the broad emission lines (BELs) is $\Delta m > 0.07$ for three BELs: CIV, CIII, and MgII. The DR12Q catalog from the Sloan Digital Sky Survey III provides five-band photometry and calibrated spectra for hundreds of thousands of quasars. These spectra include at least one emission line with a full width at half maximum $FWHM_v$ exceeding $500\,km\,s^{-1}$ or notable absorption features. Common BELs detected are CIII] $\lambda1909$, Mg II $\lambda2798$, and C IV $\lambda1549$. Given the IRT-Theseus observation band of $0.7 - 1.8\,\mu m$, and the relation $\frac{\lambda_{obs}}{\lambda_{rest}} = 1 + z$, the C IV line is observable within $2.1 < z < 13.8$; the C III] line within $1.5 < z < 11$, and the Mg II line within $0.72 < z < 7.2$. Since the IRT redshift limit is 4.5, these lines will be detectable. The broadening of BELs is caused by the Doppler effect, resulting from a distribution of velocities. The relationship between $FWHM$ in velocity and wavelength is: $\frac{c}{FWHM_v} = \frac{\lambda}{FWHM_\lambda}$. A BEL is distinguishable if $\Delta\lambda = FWHM_\lambda$ is greater than λ/R, where (R) is the spectral resolution. Using the Doppler effect, this condition is $\frac{c}{FWHM_v} < R$. For each BEL in the DR12Q catalog, we calculate $\frac{c}{FWHM_v}$ and compare it with R=400. We find that the detection probability for CIV and CIII is 100% and for MgII, it is 99.98%. Therefore, almost all BELs will be distinguishable by the IRT. Since the IRT-Theseus photometric accuracy is 5% and the corresponding $\Delta m = 0.053$, is smaller than the microlensing variability found by Fian et al.

[14], we conclude that IRT-Theseus will detect microlensing effect in lensed quasars.

4. Conclusions

In this study, we explore the capability of IRT-Theseus to detect dark matter through strong lensing of quasars. Using updated AB magnitude data and the Quasar Luminosity Function (QLF), we estimate that IRT will observe approximately $N \simeq 2.7 \times 10^5$ quasars. We also investigate quasars lensed by foreground galaxies, using new redshift distributions from the MILLIQUAS catalog. Our findings indicate that one in every 2500 quasars observed by IRT will be lensed, with about 90% of these cases involving one foreground galaxy. Additionally, we examine the microlensing effect in BELs. With a spectral resolution of R=400 and photometric accuracy of 5% we find that IRT-Theseus can detect microlensing in BELs, enhancing our understanding of quasar physics and the DM distribution of foreground galaxies.

References

[1] Vegetti, S., et al. 2023. *Strong gravitational lensing as a probe of dark matter*. arXiv preprint arXiv:2306.11781.

[2] Bertone, G., Hooper, D. and Silk, J., 2005. *Particle dark matter: Evidence, candidates and constraints*. Physics reports, 405(5-6), pp.279-390.

[3] Carr, B. and Kühnel, F., 2020. *Primordial black holes as dark matter: recent developments*. Annual Review of Nuclear and Particle Science, 70(1), pp.355-394.

[4] Mróz, P., et al. 2024. *No massive black holes in the Milky Way halo*. Nature, pp.1-2.

[5] Nierenberg, A.M., et al. 2023. *JWST lensed quasar dark matter survey I: Description and first results*. arXiv preprint arXiv:2309.10101.

[6] Hamolli, L., et al. 2023. *Investigating Gravitationally Lensed Quasars Observable by Nancy Grace Roman Space Telescope*. Galaxies, 11(3), p.71.

[7] Schneider, P., Ehlers, J. and Falco, E.,1999. *Gravitational Lenses, 1992. URL Http://books*.

[8] Shapiro, I., 1964. *Fourth test of general relativity*. Physical Review Letters, 13, 789.

[9] Vernardos, G., et al. 2024. *Microlensing of strongly lensed quasars*. Space Science Reviews, 220(1), p.14.

[10] Amati, L., et al. 2021. *The THESEUS space mission: science goals, requirements and mission concept*. Experimental Astronomy, pp.1-36.

[11] Lacy, M., et al. 2015. *The Spitzer mid-infrared AGN Survey. II. The demographics and cosmic evolution of the AGN population*. The Astrophysical Journal, 802, 102.

[12] Hamolli, L., et al. 2021. Exploiting the IRT-THESEUS capability to observe lensed Quasars. Galaxies, 9(2), p.35.

[13] Flesch, E.W., 2023. *The Million Quasars (Milliquas) Catalogue, v8*. arXiv preprint arXiv:2308.01505.

[14] Fian, C., et al. 2021. *Microlensing of the broad emission lines in 27 gravitationally lensed quasars-Broad line region structure and kinematics*. Astronomy & Astrophysics, 653, p.A109.